ELSEVIER

Signal Processing 42 (1995) 181–190

SIGNAL PROCESSING

Multifractal and generalized dimensions of gray-tone digital images

Nirupam Sarkar, B.B. Chaudhuri*

Electronics and Communication Sciences Unit, Indian Statistical Institute, 203, B.T. Road, Calcutta 700035, India

Received 19 April 1993

Abstract

Fractal geometry has found widespread applications in image processing problems. One interesting fractal parameter is the fractal dimension that characterizes the roughness of the image. Higher-order fractal dimensions called multifractal dimensions are used to characterize the underlying inhomogeneity of texture in an image. This note deals with the methods of estimating fractal and multifractal dimensions of gray-tone digital images. Experimental results on texture images from the Brodatz album are presented and discussed.

Zusammenfassung

Die Fraktal-Geometrie hat breite Anwendung auf Bildverarbeitungsprobleme gefunden. Ein interessierender Fraktal-Parameter ist die Fraktal-Dimension, die die Rauheit des Bildes charakterisiert. Fraktal-Dimensionen höherer Ordnung, genannt Multifraktal-Dimensionen, werden zur Charakterisierung der vorhandenen Inhomogenität von Mustern in einem Bild benutzt. Diese Arbeit beschäftigt sich mit Methoden zur Schätzung von Fraktal- und Multifraktal-Dimensionen von digitalen Grautonbildern. Experimentelle Ergebnisse anhand von Bildmustern aus dem Brodatz-Album werden wiedergegeben und diskutiert.

Résumé

La géométrie fractale a trouvé de nombreuses applications dans les problèmes de traitement d'images. Un paramètre fractal intéressant est la dimension fractale qui caractérise la rugosité d'une image. Les dimensions fractales d'ordre supérieur, appelées dimensions multi-fractales, sont utilisées pour caractériser l'inhomogénéité sous-jacente de la texture présente dans une image. Cet article est consacré aux méthodes d'estimation des dimensions fractale et multi-fractales d'images numériques à niveaux de gris. Des résultats expérimentaux sur des images de texture tirées de l'album Brodatz sont présentés et commentés.

Keywords: Fractal; Multifractal; Texture analysis; Generalized dimension; Box counting approach; Feature extraction

1. Introduction

Simple objects can be described by the ideal shape primitives, such as cubes, cones or cylinders. But most of the natural objects are so complex and erratic that they cannot be described in terms of simple primitives. The phenomenon of resolution dependence of measures emerges in nearly all quantitative tasks of image analysis. Fractal geometry supplies the theoretical basis to describe this

*Corresponding author.

SSDI 0165-1684(94)00126-X

phenomenon. If a scaling exponent of an object remains constant over a certain range of resolution, the object is said to be self-similar. Self-similarity can be characterized by a parameter called fractal dimension. The complex and erratic shape description in terms of self-similarity was introduced by Mandelbrot [12].

The concept of fractal dimension (FD) can be useful in the measurement, analysis and classification of shape and texture. Pentland [15, 16] noticed that the fractal model of imaged three-dimensional (3D) surfaces can be used to obtain shape information and to distinguish between smooth and rough textured regions. Rigaut [18] used the concept for image segmentation. Some of the other applications involve sedimentology and particle morphology [13, 10], image data compression [1, 8] and computer graphics [21].

Fractal dimension is used to characterize systems with self-similarity of simple and homogeneous fractals. FD is not enough for characterization of sets having non-isotropic and inhomogeneous scaling properties. For such a characterization one has to generalize the analysis using the concept of multifractals which implies a continuous spectrum of exponents for the characterization of the system. In this generalization, an inhomogeneous fractal set is considered to be interwoven with infinitely many sub-fractal sets of different dimensions.

Blacher et al. [2] used multifractals to characterize the morphology of polymer alloys and granular discontinuous thin film. Kanmani et al. [9] used multifractal formalism in describing the inhomogeneity of stress corrosion crack patterns. Chaudhuri et al. [4] used multifractals of order 2 along with other fractal features for texture segmentation.

Blacher et al. [2] and Kanmani et al. [9] estimated generalized dimensions for two-tone images. We have not come across any work of estimating the generalized dimension of gray-tone texture images.

In this paper we propose an algorithm to compute the generalized dimension of gray-tone digital images. The basics of FD and different approaches of its estimation are reviewed in Section 2. The estimation procedure of generalized dimension (GD) is presented in Section 3. In Section 4 the special case of two-tone images is described. This section also contains the results of using the proposed algorithm on texture images and related discussions.

2. Estimation of fractal dimension

2.1. Background

The Hausdorff–Besicovitch dimension of a bounded set A in $\mathbb{R}^n$ is a real number used to characterize the geometrical complexity of A.

Consider the metric space $(\mathbb{R}^n, d)$, where n is a positive integer and d denotes the Euclidean metric. Let $A \subset \mathbb{R}^n$ be bounded. The diameter of A is defined as

$$\operatorname{diam}(A) = \sup\{d(x, y)\colon x, y \in A\}.$$

Let $0 < \varepsilon < \infty$; $0 \leqslant p < \infty$. Let $\mathscr{A}$ denote the set of sequences of subsets $\{A_i \subset A\}$, such that $A = \bigcup_{i=1}^{\infty} A_i$. Then we define the *Hausdorff p-dimensional outer measure* of A as

$$\mu_{p,\varepsilon}(A) = \inf\left\{ \sum_{i=1}^{\infty} [\operatorname{diam}(A_i)]^p \colon \{A_i\} \in A, \text{ and } \operatorname{diam}(A_i) < \varepsilon \quad \text{for } i = 1, 2, 3, \ldots \right\}.$$

Note that $\mu_{p,\varepsilon}$ is non-decreasing as ε decreases. Let $\mu_p(A) = \lim_{\varepsilon \downarrow 0} \mu_{p,\varepsilon}(A)$. The Hausdorff–Besicovitch dimension (D_{H}) is defined as

$$D_{\mathrm{H}} = \sup\{p \in \mathbb{R}\colon p > 0,\ \mu_p(A) = \infty\},$$

where it is assumed that $\sup \phi = 0$.

A set is called a fractal set if its Hausdorff–Besicovitch dimension is strictly greater than its topological dimension. Mandelbrot [12] coined the term fractal from the Latin word *fractus*, which means irregular segments.

The Hausdorff–Besicovitch dimension is often called the fractal dimension (FD). Mandelbrot [12] defined FD in the following way.

Let $A \in \mathbb{R}^n$. For each $\varepsilon > 0$ let $\mathscr{N}(A, \varepsilon)$ denote the smallest number of closed balls of radius ε needed to cover A. If for a constant C

$$\mathscr{N}(A, \varepsilon) = C\varepsilon^{-D} \tag{1}$$

exists, then D is called the *fractal dimension* of A.

Mandelbrot proposed an approach to calculate FD while estimating the length of a coastline. Consider all points with distances to the coastline of not greater than ε. These points form a strip of width 2ε, and the suggested length $L(\varepsilon)$ of the coastline is the area of the strip divided by 2ε. As ε decreases, $L(\varepsilon)$ increases. The length $L(\varepsilon)$ can be obtained from Eq. (1) as

$$L(\varepsilon) = F\varepsilon^{1-D}. \tag{2}$$

The fractal dimension (FD) of the line D can be derived from the least-squares linear fit of the plot of $\log L(\varepsilon)$ versus $\log \varepsilon$. If m is the slope of the fitted line then FD of the curve (coastline) is given by $1 - m$. Note that m is a negative real number in the range of 0–1 and $1 \leqslant D \leqslant 2$.

There exist several approaches to estimate the FD in an image. For example, Peleg et al. [14] used the ε-blanket method which is a 2-D generalization of the original approach suggested by Mandelbrot [12]. Pentland [15, 16] considered the image intensity surface as a fractal Brownian function (fBf) and estimated FD from the Fourier power spectrum of fBf. Gangepain and Roques-Carmes [6] as well as Keller et al. [11] used variations of the box counting approach to estimate FD.

Of these methods, those due to Peleg et al. and Pentland give accurate results, but they are computationally expensive. On the other hand, the methods due to Gangepain and Roques-Carmes as well as Keller et al. are accurate for only a small portion of the dynamic range of FD, although they are computationally efficient. Here we present a computationally efficient method that gives accurate results over the full dynamic range of FD. The method, called differential box counting (DBC) method [19], is described below.

2.2. DBC estimation of fractal dimension

The concept of self-similarity can also be used to estimate the fractal dimension. A bounded set A in Euclidean n-space is self-similar if A is the union of N_r distinct (non-overlapping) copies of itself scaled down by a ratio r. Fractal dimension D of A is given by the relation [12]

$$1 = N_r r^D \quad \text{or} \quad D = \frac{\log(N_r)}{\log(1/r)}. \tag{3}$$

However, natural scenes practically do not exhibit deterministic self-similarity. Instead, they exhibit some statistical self-similarity. Thus, if a scene is scaled down by a ratio r in all n dimensions, then it becomes statistically identical to the original one, so that Eq. (3) is satisfied.

In the DBC method, N_r is counted in the following manner. Consider that the image of size $M \times M$ pixels has been scaled down to a size $s \times s$ where $M/2 \geqslant s > 1$ and s is an integer. Then we have an estimate of $r = s/M$. Now, consider the image as a 3-D space with (x, y) denoting 2-D position and the third co-ordinate (z) denoting the gray level. The (x, y) space is partitioned into grids of size $s \times s$. On each grid there is a column of boxes of size $s \times s \times s'$. If the total number of gray levels is G then $\lfloor G/s' \rfloor = \lfloor M/s \rfloor$. See, for example, Fig. 1 where $s = s' = 3$. Assign numbers 1, 2, ... to the boxes as shown. Let the minimum and maximum gray level of the image in the (i,j)th grid fall in the box numbered k and l, respectively. Then

$$n_r(i,j) = l - k + 1 \tag{4}$$

is the contribution of N_r in the (i,j)th grid. For example, in Fig. 1 $n_r(i,j) = 3 - 1 + 1$. Taking contributions from all grids, we have

$$N_r = \sum_{i,j} n_r(i,j). \tag{5}$$

N_r is counted for different values of r (i.e. different values of s). Then using (3) we can estimate D, the fractal dimension, from the least-squares linear fit of $\log(N_r)$ against $\log(1/r)$. Because of the differential nature of $n_r(i,j)$, we call the method as differential box counting method.

In actual implementation, a random placement of boxes is done to reduce the quantization effect of the approach. More specifically, the column of boxes are given random shift in units of gray value along the x-direction although the box size remains the same. Shifts in the x- or y-direction are also done in multiples of pixel length/breadth [20]. As explained in [20], such random placement makes a better estimate of FD for images with periodic spatial structures. See Fig. 2 for horizontal shift in

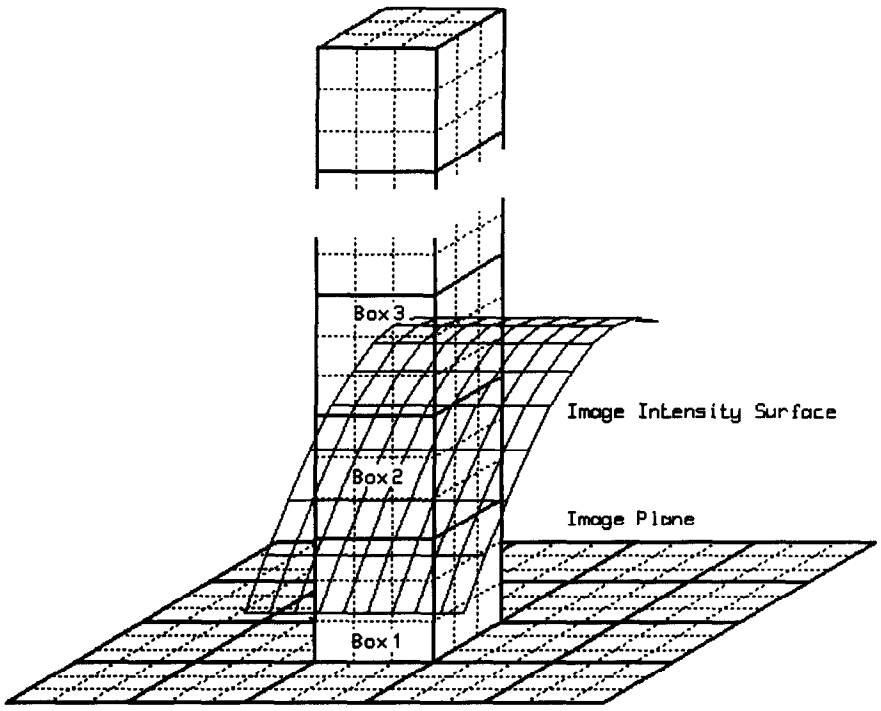

Fig. 1. Determination of n_r by the proposed method.

the x-direction. Vertical shift can be made in an identical way.

An algorithm to estimate FD using the DBC approach is as follows.

Algorithm FD

$s = 2$
while ($s <$ level)
  for $s = 2$ to $s_{\max}$
  $N_r = 0$
  for *all boxes* do
    $min \leftarrow$ minimum gray value of the points of current box
    $max \leftarrow$ maximum gray value of the points of current box
    $n_r \leftarrow max - min + 1$
  $N_r \leftarrow N_r + n_r$
Call $LINFIT(\log N_r, \log(1/r), m, c)$ {$LINFIT$ is the subroutine to fit a line returning the slope m and ordinate intercept c of the fitted line}
$D = m$.
End.

Next we shall consider the generalized dimension D_q and see that D_0 is equivalent to D described here.

3. Multifractals and generalized dimension

The properties of self-similarity of a set of points can be characterized by fractal dimension. Note that only for simple cases can this be considered as an exhaustive characterization. For non-isotropic or inhomogeneous scaling properties, the sets require a more general treatment and one has to generalize the analysis using the concepts of multifractals which implies a continuous spectrum of exponents for the systems characterization. During the last few years it has been demonstrated that the multifractals are necessary to characterize the properties of various physical phenomena like turbulence, strange attractors in general, fractal growth models, multiplicative processes, and others.

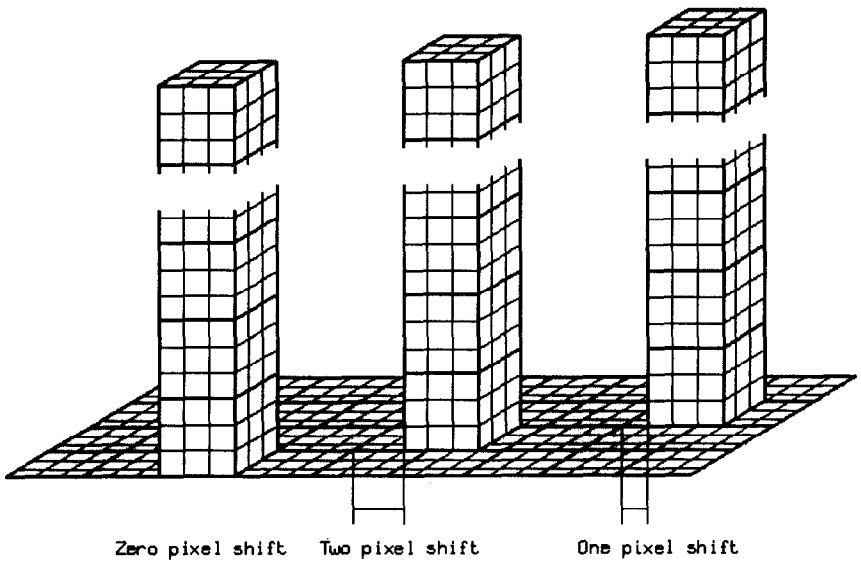

Fig. 2. Column shifting in the x-direction.

3.1. Generalized dimension

In computing the box counting dimension, one counts the non-empty boxes without any regard to the number of points in a box, i.e. no weighting is done to the count according to the number of points in the box. This approach describes the geometry of the structure but ignores the underlying measure, i.e. the density of the point distribution over it. A measure defined over a set describes the varying density of a positive scalar quantity like mass.

The generalized dimension introduced by Grassberger [7] takes into account the number of points in a box. Let B_i denote the ith box. Then $u(B_i)$ is the measure defined for the ith box and is equal to the number of points within the box. Also, $u(A)$ is the total measure of the set A and is equal to the total number of points in the set A. Then $P_i = u(B_i)/u(A)$ is the normalized measure of the ith box. The generalized dimension is given as

$$D_q = \frac{1}{q-1}\lim_{r\to 0}\frac{\log\sum_i^{N_r} P_i^q}{\log r}, \tag{6}$$

where $-\infty \leqslant q \leqslant \infty$ and N_r denotes the non-empty boxes.

For a homogeneous fractal, with all the P_i being equal, one obtains the generalized dimension D_q, which does not vary with q. But in the case of an inhomogeneous fractal, D_q usually decreases with increasing q. Note that D_0 computed using Eq. (6) is equivalent to the FD of the set A.

Coleman and Pietrinero [5] defined a partition function as

$$\chi(q,r) = \sum_i P_i^q \propto r^{\tau(q)}.$$

The role of this function is to evaluate all the possible singularities of the distribution by studying all the q moments of the coarse grained distribution for different sized coarse graining. The exponent $\tau(q)$ defines the small r behavior of $\chi(q,r)$. Even a regular distribution can be characterized in this way. Their non-fractal properties would arise from a particular behavior of $\tau(q)$. The generalized dimension D_q can be defined as

$$(q-1)D_q \equiv \tau(q) = \lim_{r\to 0}\frac{\ln\chi(q,r)}{\ln r}. \tag{7}$$

Applying L'hospital in Eq. (6) we get

$$D_1 = \lim_{r\to 0}\frac{\sum_i P_i \log P_i}{\log r}.$$

D_1 is called the information dimension. Note that the numerator term in the expression of D_1 is identical to classical information measure if P_i denotes

probability. D_2 is called the correlation dimension which is a measure of correlation between pairs of points inside a box. For $q = 3, 4, \ldots$ one can define a set of generalized dimensions D_3, D_4 associated with higher-order correlations between triples, quadruples, of points in each box [2].

3.2. Box counting approach

In this paper generalized dimensions (GD) of texture images are estimated, which is more difficult than finding the GD of a two-tone image described in Section 4. At first, image intensity surface is constructed from the given image by connecting the neighboring image points in 3-D. For a given box size s the image is partitioned into boxes of size $s \times s \times s'$. Let B_{ijk} denote the (i,j,k)th box. Let $u(B_{ijk})$ be the number of points counted at B_{ijk}.

The total number of points of the image intensity surface is given by

$$u(A) = \sum_{\forall i,j,k} u(B_{ijk}),$$

then $P_{ijk} = u(B_{ijk})/u(A)$.
Let $\chi(q,r) = \sum_{ijk} P_{ijk}^q$. Then the 3-D generalization of Eq. (6) can be given as

$$D_q = \frac{1}{q-1} \lim_{r \to 0} \frac{\log \chi(q,r)}{\log r} \quad (q \neq 1), \tag{8}$$

$$D_1 = \lim_{r \to 0} \frac{\sum_i P_i \log P_i}{\log r},$$

where $r = s/M$ as given in Section 2.2.

For a given value of q, $\chi(q,r)$ is computed for different values of r and D_q is estimated from the plot of $\log \chi(q,r)$ against $\log r$.

The most important part in this method is the image intensity surface approximation and counting of $u(B_{ijk})$. The approximation is done at first for all columns of the image where the neighboring gray value points (in 3-D space) are joined by straight lines. Then the same process is done for all rows. For counting, at first the 3-D space is partitioned into boxes of size $s \times s \times s'$, then the number of points in the (i,j,k)th box is counted as $u(B_{ijk})$. Note that for a given value of s one can have a maximum count of $s \times s \times s'$ for $u(B_{ijk})$.

An algorithm to find the generalized dimension is as follows.

Algorithm for GD(q)
{for image of size $M \times M$, image function denoted by $f[i,j]$ and 3-D matrix denoted by $F[i,j,k]$}
for $i = 0$ to $M-1$
for $j = 0$ to $M-1$
for $k = 0$ to $G-1$ /*G is the number of gray levels */
  $F[i,j,k] = 0$
for $i = 0$ to $M-1$
for $j = 0$ to $M-2$
  join $(i,j,f[i,j])$ and $(i,j+1,f[i,j+1])$ of F matrix by a straight line
for $j = 0$ to $M-1$
for $i = 0$ to $M-2$
  join $(i,j,f[i,j])$ and $(i+1,j,f[i+1,j])$ of F matrix by a straight line
for $s = 2$ to S_{max}
Initialize $N(q,r)$ for all q and $\chi(1,r)$
for $i = 0$ to $M/s-1$
for $j = 0$ to $M/s-1$
  Initialize Temp(q) for all q {'Temp(q)' is a temporary array}
  for $k = 0$ to $M/s-1$
    $N_k \leftarrow$ number of points B_{ijk}
    $\chi(1,r) \leftarrow \chi(1,r) + N_k \log N_k$
    Temp(q) $\leftarrow$ Temp(q) $+ N_k^q$
  $N(q,r) \leftarrow N(q,r) +$ Temp(q)
$\chi(1,r) \leftarrow \chi(1,r)/N(1,r) - \log N(1,r)$
Normalize $N(q,r)$ to get $\chi(q,r)$ $(q \neq 1)$
For all q $(q \neq 1)$
  Call $LINFIT(\log \chi(q,r), \log(r), m, c)$
  $\tau_q = m$
  $D_q = \dfrac{\tau_q}{q-1}$
Call $LINFIT(\chi(1,r), \log r, m, c)$
$D_1 = m$
End

4. Results and discussion

We compare the DBC method with four other methods due to Peleg et al. [14], Pentland [15], Gangepain and Roques-Carmes [6], and Keller et al. [11]. The algorithms are tested on the

synthetic images which are actually zero-mean Gaussian noise with standard deviation σ added to an absolutely smooth image surface at gray level 128. Suitable truncation is done so that the resulting gray levels lie in the range 0–255. It is expected that the FD will increase if the noise σ increases, and beginning at 2.0 the FD will asymptotically go towards a value of 3.0. A good estimation method should reflect this desirable feature.

The results are plotted in Fig. 3. It is seen that the method due to Pentland, Peleg et al. and the DBC approach give satisfactory results. On the other hand, methods due to Gangepain and Roques-Carmes and Keller et al. give satisfactory results up to a certain level of roughness of the image intensity surface. After a certain value of FD, which is 2.5 and 2.75 for the methods due to Gangepain and Roques-Carmes [6] and Keller et al. [11], respectively, the slope of the curve nearly goes to zero and hence these methods do not cover the full dynamic range of FD. Similar behavior is observed on other real images from the Brodatz [3] album.

Let the image function be $f(x, y)$. Consider the plot $x, y, f(x, y)$ in a 3-D space for all x and y. Now, if the generalized dimension of the above space is estimated without the space approximation described in Section 3.2 then for $q = 0$ the estimated value of D_0 will be equal to the FD estimated using the Gangepain and Roques-Carmes [6] method. On the other hand, if the surface approximation is made, then the estimated D_0 is similar to the FD estimated by the DBC method and here D_0 covers the full dynamic range of FD.

However, due to insufficiency of memory the image intensity surface approximation of the whole image may not be done at one time. To solve this problem surface approximation can be done locally. For example, if we want to calculate $u(B_{ijk})$ where the box size is s, then the following steps should be taken.

Step 1. Join $f(i*s + l, j*s + m)$ and $f(i*s + l, j*s + m + 1)$ for $0 < l < s$, $1 < m < s$.

Step 2. Join $f(i*s + l, j*s + m)$ and $f(i*s + l + 1, j*s + m)$ for $1 < l < s$, $0 < m < s$.

Step 3. Count $u(B_{ijk})$ as number of points in box (i, j, k).

To complete the study, it may be useful to discuss the approaches to compute FD of two-tone images. There exist many algorithms for the purpose, although these algorithms were originally meant for finding the FD of curves.

The most widely used definitions of dimension of this class are the Minkowski–Bouligand dimension and the box dimension. These are described by Mandelbrot [12]. Although they are equivalent in the limiting case, in practice they give rise to algorithms that behave quite differently.

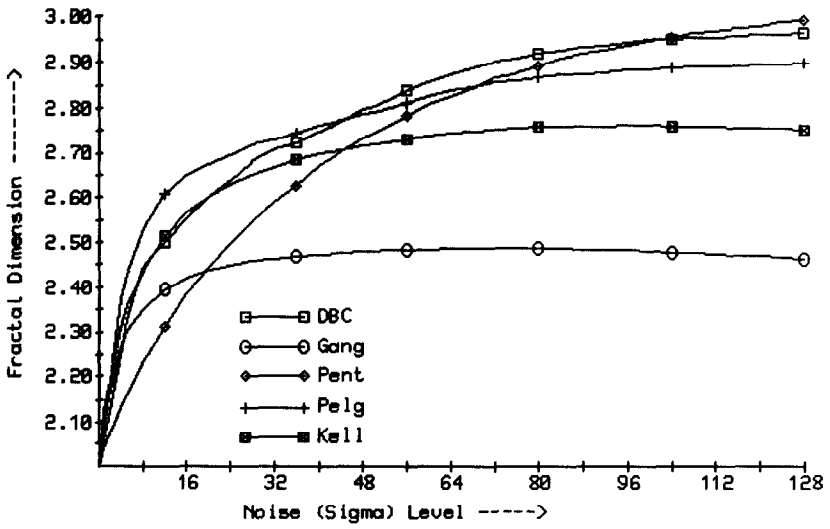

Minkowski–Bouligand dimension: The *Minkowski* cover of a set E is the set of all points $E(\varepsilon)$ defined as follows:

$$E(\varepsilon) = \{y: y \in B_\varepsilon(x)\}, \quad x \in E,$$

where B_ε is a disk of radius ε centered on x. In other words, $E(\varepsilon)$ consists in the union of all the disks centered on E, with radius ε. The area of the Minkowski cover is E_ε. From the log–log plot of $(1/\varepsilon)$ and E_ε an estimate of $2 - D$ is found where D is the FD of the curve.

Box dimension: The two-tone image is partitioned into touching squares of size $s \times s$. Now, the number of non-empty boxes are counted as N_r ($r = s/M$, where image size is $M \times M$), which is equivalent to the number of boxes needed to cover the image. Then the following equation holds good:

$$1 = N_r r^D,$$

where D is the fractal dimension of the image and is estimated from the log–log plot of N_r and $1/r$.

Barnsley [1] and Mandelbrot [12] used these methods to find the FD of two-tone synthetic fractal images. Pickover and Khorasani [17] used the box counting method to find FD to characterize speech wave graphs.

Blacher et al. [2] studied multifractal behavior of granular evaporated thin gold films of different gold concentration. They made the following observations from the plot of D_q versus q for different gold concentration. For the smallest concentration, with non-connected morphology, the generalized dimension decreases linearly with q. For high concentration the curve tends toward a constant D_q, indicating a more uniform feeling of the plane. Multifractality means non-uniform fractal, and the greater the difference between D_0 and the other dimension D_q, the more non-uniform is the

Fig. 4. Natural textures [3].

Table 1
Generalized dimensions of different texture images

Image	D_0	D_1	D_2	D_3	D_4	D_5	D_6	D_7	D_8	D_9
D03	2.68	2.35	2.35	2.35	2.34	2.33	2.32	2.31	2.30	2.29
D04	2.72	2.52	2.54	2.53	2.53	2.52	2.51	2.50	2.50	2.49
D05	2.63	2.46	2.48	2.48	2.48	2.47	2.46	2.46	2.45	2.44
D06	2.39	2.38	2.41	2.42	2.42	2.41	2.40	2.39	2.38	2.37
D09	2.66	2.44	2.47	2.47	2.47	2.47	2.46	2.46	2.45	2.45
D12	2.53	2.42	2.44	2.45	2.45	2.45	2.45	2.45	2.44	2.44
D17	2.66	2.52	2.53	2.52	2.51	2.49	2.48	2.47	2.45	2.44
D20	2.66	2.57	2.58	2.58	2.58	2.56	2.55	2.54	2.53	2.52
D21	2.62	2.70	2.72	2.72	2.72	2.71	2.70	2.68	2.67	2.66
D24	2.53	2.41	2.44	2.45	2.45	2.44	2.44	2.43	2.43	2.42
D28	2.63	2.33	2.37	2.38	2.39	2.39	2.39	2.38	2.38	2.38
D33	2.32	2.29	2.30	2.30	2.30	2.29	2.29	2.28	2.28	2.27
D34	2.26	2.14	2.16	2.17	2.17	2.17	2.17	2.17	2.16	2.16
D51	2.53	2.21	2.25	2.29	2.33	2.35	2.36	2.37	2.37	2.37
D54	2.47	2.31	2.33	2.34	2.34	2.34	2.33	2.33	2.33	2.32
D55	2.56	2.32	2.35	2.36	2.36	2.36	2.35	2.35	2.34	2.34
D65	2.40	2.24	2.26	2.26	2.26	2.26	2.26	2.25	2.25	2.25
D68	2.59	2.44	2.47	2.48	2.48	2.48	2.47	2.47	2.47	2.46
D77	2.74	2.65	2.66	2.65	2.63	2.62	2.61	2.59	2.58	2.57
D82	2.53	2.46	2.49	2.50	2.49	2.49	2.48	2.47	2.47	2.46
D84	2.67	2.43	2.45	2.45	2.44	2.44	2.43	2.42	2.41	2.41
D92	2.57	2.45	2.48	2.49	2.49	2.48	2.48	2.47	2.47	2.46
D101	2.70	2.46	2.48	2.48	2.48	2.48	2.48	2.47	2.46	2.46

structure. Kanmani et al. [9] studied the multifractal behavior of stress corrosion cracks. They observed that the curve of D_q versus q indicates the inhomogeneity of the cracks. Multifractal behavior of a textural image is somewhat complicated than binary image. Textures can be described by its basic properties such as coarseness, uniformity, roughness and directionality. Some of these properties can be described by the generalized dimension of the texture. We stated earlier that FD reflects the roughness of a texture. It has been observed that for very fine structured texture (e.g. D21), D_2 is a little higher than D_0, which will not occur in the case of binary image. Usually, the value of $D_0 - D_2$ reflects the coarseness of the grain of the texture. It has also been observed that as we increase the value of q, D_q saturates to a certain value for a given texture, indicating the limit of fractal non-uniformity of texture image. It is observed that for fine texture the curve of D_q versus q is more or less straight. Similar behavior is observed by Blacher [2], on the image of gold film with low gold concentration. However, the characteristics of D_1 for texture images is under

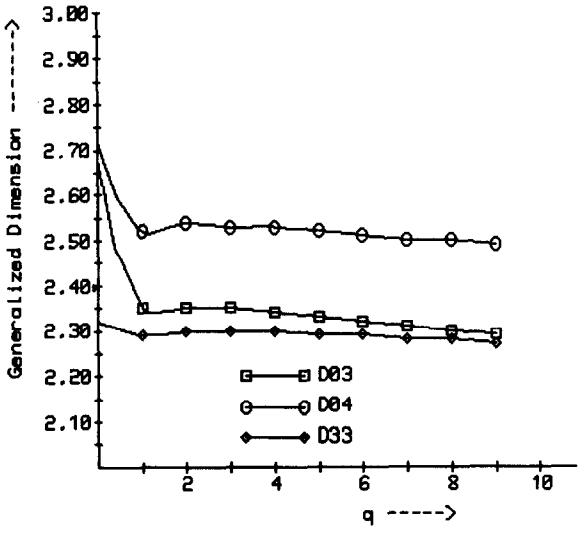

further study. Typical textures used for the computation of FD of different order are shown in Fig. 4. These images are taken from the Brodatz [3] album. The results are shown in Table 1 and Fig. 5.

References

[1] M.F. Barnsley, *Fractal Everywhere*, Academic Press, San Diego, CA, 1988.

[2] S. Blacher, F. Brouers and G. Ananthakrishna, "Multifractal analysis of real heterogeneous materials", in: *Proc. 11th ACTA Stereol*, Irvine, CA, 1992. pp. 349–354.

[3] P. Brodatz, *Texture: A Photographic Album for Artists and Designers*, Dover, New York, 1966.

[4] B.B. Chaudhuri, N. Sarkar and P. Kundu, "An improved fractal geometry based texture segmentation technique", *Proc. IEE Part E*, in press.

[5] P.H. Coleman and L. Pietronero, "The fractal structure of the universe", *Phys. Report*, Vol. 213, 1992, pp. 311–391.

[6] J.J. Gangepain and C. Roques-Carmes, "Fractal approach to two dimensional and three dimensional surface roughness", *Wear*, Vol. 109, 1986, pp. 119–126.

[7] P. Grassberger, "Generalized dimension and strange attractors", *Phys. Lett. A.* Vol. 97, 1983, pp. 227–230.

[8] A.L. Jacquin, A fractal theory of iterated Markov operators, with applications to digital image coding, Ph.D. Thesis, Dept. Mathematics, Georgia Inst. of Tech., 1989.

[9] S. Kanmani, C.B. Rao, D.K. Bhattacharjee and B. Raj, "Multifractal analysis of stress corrosion cracks", in: *Proc. 11th ACTA Stereol*, Irvine, CA, 1992, pp. 349–354.

[10] B.H. Kaye, "Fractal dimension and signature waveform characterization of fine particle shape", *Amer. Lab.*, 1986, pp. 55–63.

[11] J. Keller, R. Crownover and S. Chen, "Texture description and segmentation through fractal geometry", *Comput. Vision Graph. Image Process.*, Vol. 45, 1989, pp. 150–160.

[12] B.B. Mandelbrot, *Fractal Geometry of Nature*, Freeman Press, San Francisco, 1982.

[13] J.D. Orford and W.B. Whalley, "The use of fractal dimension to characterize irregular-shaped particle", *Sedimentology*, Vol. 30, 1983, pp. 655–668.

[14] S. Peleg, J. Naor, R. Hartley and D. Avnir, "Multiple resolution texture analysis and classification", *IEEE Trans. Pattern Anal. Machine Intell.*, Vol. PAMI-6, 1984, pp. 518–523.

[15] A.P. Pentland, "Fractal based description of natural scenes", *IEEE Trans. Pattern Anal. Machine Intell.*, Vol. PAMI-6, 1984, pp. 661–674.

[16] A.P. Pentland, "Shading into texture", *Artificial Intelligence*, Vol. 29, 1986, pp. 147–170.

[17] C. Pickover and A. Khorasani, "Fractal characterization of speech waveform graphs", *Comput. Graph.*, Vol. 10, 1986, pp. 51–61.

[18] J.P. Rigaut, "Automated image segmentation by mathematical morphology and fractal geometry", *J. Microscopy*, Vol. 150, 1988, pp. 21–30.

[19] N. Sarkar and B.B. Chaudhuri, "An efficient approach to estimate fractal dimension of texture image", *Pattern Recognition*, Vol. 25, 1992, pp. 1035–1041.

[20] N. Sarkar and B.B. Chaudhuri, "An efficient differential box counting approach to compute fractal dimension in image", *IEEE Trans. System Man Cybernetics*, in press.

[21] G. Zorpette, "Fractal: Not just another pretty picture", *IEEE Spectrum*, Vol. 25, 1988, pp. 29–31.